Bone 154 (2022) 116252

Contents lists available at ScienceDirect

Bone

journal homepage: www.elsevier.com/locate/bone

Bone microstructure in healthy men measured by HR-pQCT: Age-related changes and their relationships with DXA parameters and biochemical markers

Mitsuru Doi, Ko Chiba *, Narihiro Okazaki, Choko Kondo, Shuta Yamada, Kazuaki Yokota, Akihiko Yonekura, Masato Tomita, Makoto Osaki

Department of Orthopedic Surgery, Nagasaki University Graduate School of Biomedical Sciences

ARTICLE INFO

Keywords:
High-resolution peripheral quantitative computed tomography (HR-pQCT)
Male osteoporosis
Bone microstructure
Dual-energy X-ray absorptiometry
Bone turnover marker

ABSTRACT

Objective: The primary purpose of this cross-sectional study was to investigate the characteristics of age-related changes in bone microstructure on high-resolution peripheral quantitative computed tomography (HR-pQCT), areal bone mineral density (aBMD) on dual-energy X-ray absorptiometry (DXA), and bone-related biochemical markers in men. The secondary purpose of this study was to examine how bone microstructure is related to aBMD and biochemical markers.

Methods: The subjects were 128 healthy Japanese men (20–97 years old). Bone microstructure was measured in the distal radius and tibia using second-generation HR-pQCT; aBMD in the proximal femur and lumbar spine was measured with DXA; and tartrate-resistant acid phosphatase-5b (TRACP-5b), type I procollagen-N-propeptide (P1NP), 25(OH) vitamin D, and pentosidine concentrations were measured by blood tests.

Results: In trabecular bone, the trabecular volumetric BMD (Tb.vBMD) and trabecular number (Tb.N) were lower with age ($r = -0.23, -0.35$) ($r = -0.36, -0.33$), and trabecular separation (Tb.Sp) and the star volume of marrow space (V*ms) were higher with age ($r = 0.29, 0.41$) ($r = 0.34, 0.38$) in both the radius and tibia.

In cortical bone, cortical volumetric BMD (Ct.vBMD) was lower with age ($r = -0.25, -0.52$), and cortical porosity (Ct.Po) was higher with age ($r = 0.67, 0.62$) in both the radius and tibia. In the tibia, cortical thickness (Ct.Th) and cortical area (Ct.Ar) were lower with age ($r = -0.40$) ($r = -0.43$), whereas, in the radius, they were maintained, and periosteal perimeter (Ct.Pm) was higher with age ($r = 0.35$).

aBMD in the proximal femur and P1NP were lower, and pentosidine was higher with increased age, whereas aBMD in the lumbar spine, TRACP-5b, and 25(OH) vitamin D had no relationships with age.

DXA and HR-pQCT showed strong correlations particularly with femoral aBMD and tibial Tb.vBMD and Ct.Ar ($r = 0.61$) ($r = 0.61$), whereas no DXA parameters were related with Ct.Po. In correlations between biochemical markers and HR-pQCT, TRACP-5b and total P1NP were negatively correlated with Ct.vBMD ($r = -0.31$) ($r = -0.35$), but almost no other correlations were seen.

Conclusions: Age-related changes of the bone microstructure in men were characterized by decreases in trabecular and cortical vBMD associated with decreased trabecular number, cavitation of the trabecular structure, and increased cortical porosity. Femoral aBMD was strongly related to bone microstructure in the tibia, whereas both lumbar aBMD and femoral aBMD were not related to Ct.Po, and biochemical markers showed almost no relationships with bone microstructure.

1. Introduction

Osteoporosis is defined as a skeletal disorder characterized by compromised bone strength predisposing a person to an increased risk of fracture. Bone strength primarily reflects the integration of bone density and bone quality [1,2].

In men with osteoporosis, the prognosis is generally poor, and the mortality rate after a fragility fracture is higher than that in women;

* Corresponding author at: Department of Orthopedic Surgery, Nagasaki University Graduate School of Biomedical Sciences, 1-7-1 Sakamoto, Nagasaki 852-8501, Japan.
E-mail address: kohchiba@estate.ocn.ne.jp (K. Chiba).

https://doi.org/10.1016/j.bone.2021.116252
Received 15 May 2021; Received in revised form 30 October 2021; Accepted 1 November 2021
Available online 4 November 2021

Table 1
Background information of the participants and measurement values of DXA parameters, biochemical markers, and their correlations with age, change (%) over 10 years, and comparisons among generations.

Variable	Total	Correlation with age	Change (%) in 10 years	Age (20–29 y)	(30–39 y)	(40–49 y)	(50–59 y)	(60–69 y)	(70–79 y)	(≥80 y)
Number	128			20	19	20	19	20	20	10
Age (y)	53.5 (36.0–69.0)			24.5 (21–27.8)	35.0 (32–36)	45(42–48)	55.0 (53–57)	64.5 (61–67.8)	74.5 (71.5–77)	83.0 (81.8–84.5)
Height (cm)	169 (164–173)	**−0.465****	−0.96	171 (168–175)	170 (168–175)	172 (178–178)	169 (166–171)	169 (166–172)	**162 (160–165)**[abc]	**163 (156–167)**[abc]
Weight (kg)	65.5 (60.0–74.0)	**−0.236****	−1.69	65.0 (62–73)	66.0 (59–75)	72.5 (62–80)	72.5 (69–81)	65.0 (59–71)	62.0 (56–68)[cd]	58.0 (55–64)[cd]
BMI (kg/m^2)	23.3 (21.6–25.3)	0.040	0.15	22.6 (19.8–24.1)	22.7 ± 3.0	24.2 (21.2–26.7)	26.0 (23.2–28.3)	22.8 (21.4–24.5)	23.5 (21.8–24.4)	22.5 (22.0–23.2)
CKD (stage 3)	27 (21.1)			0 (0)	1 (5.3)	0 (0)	6 (31.6)	5 (25.0)	8 (40.0)	7 (70.0)
Type2 DM	6 (4.7)			0 (0)	0 (0)	0 (0)	1 (5.3)	2 (10.0)	2 (10.0)	1 (10.0)
Exercise frequency (0/1-2/3-4/5-7 days per week)	49/40/25/14			8/6/4/2	7/8/3/1	10/6/3/1	10/4/4/1	4/7/5/4	8/4/4/4	2/5/2/1
Total hip (g/cm^2)	0.98 (0.88–1.08)	**−0.328****	−2.68	1.13 (1.03–1.24)	1.00 (0.90–1.07)	0.94 (0.87–1.06)	0.99 (0.92–1.06)	**0.95 (0.86–1.03)**[a]	0.94 (0,85–1.10)[a]	0.92 (0.81–1.04)[a]
Femoral neck (g/cm^2)	0.90 (0.82–1.04)	**−0.459****	−3.71	1.11 (1.02–1.18)	0.95 (0.88–1.08)	**0.89 (0.82–1.03)**[a]	**0.91 (0.81–0.98)**[a]	**0.89 (0.79–0.95)**[a]	**0.86 (0.79–1.00)**[a]	**0.83 (0.73–0.92)**[a]
Lumbar spine (g/cm^2)	1.14 (1.03–1.29)	0.081	1.20	1.20 (1.14–1.29)	1.11 (1.01–1.17)	1.07 (1.00–1.16)	1.14 (1.05–1.22)	1.21 (1.04–1.39)	1.14 (1.00–1.40)	1.17 (1.03–1.38)
Osteopenia (T-score < −1)	48 (37.5)			2 (10.0)	4 (21.1)	8 (40.0)	8 (42.1)	10 (50.0)	11 (55.0)	5 (50.0)
Osteoporosis (T-score ≤ −2.5)	5 (3.9)			0 (0)	0 (0)	1 (5.0)	1 (5.3)	0 (0)	1 (5.0)	2 (20.0)
cCa (mg/dL)	9.4 (9.1–9.7)	**−0.466****	−0.95	9.7 (9.3–9.8)	9.7 (9.4–9.9)	9.4 (9.0–9.7)	9.4 (9.2–9.5)	**9.2 (9.0–9.4)**[ab]	9.2 (9.1–9.3)[b]	9.2 (9.0–9.3)[b]
P (mg/dL)	3.3 (2.9–3.7)	**−0.285****	−2.18	3.5 (3.1–3.9)	3.8 (3.3–4.0)	3.1 (2.8–3.4)[b]	3.3 (2.9–3.7)	3.3 (2.8–3.5)	3.2 (2.9–3.6)	3.1 (2.8–3.5)
TRACP-5b (mU/dL)	325 (263–383)	−0.092	−0.40	379 (321–431)	313 (263–367)	305 (260–357)	314 (217–370)	390 (294–445)	306 (251–342)	292 (235–442)
total P1NP (μg/L)	43.3 (33.7–53.9)	**−0.493****	−12.39	73.9 (55.2–101)	53.0 (46.6–67.4)[a]	**39.5 (30.2–51.0)**[a]	**41.4 (34.5–48.4)**[a]	**40.3 (33.2–43.8)**[a]	**37.8 (27.5–46.7)**[a]	**36.3 (29.8–42.1)**[a]
25(OH) vitamin D (ng/mL)	16.9 (13.3–21.5)	0.147	2.47	17.6 (10.621.2)	15.8 (12.7–19.4)	15.0 (12.0–18.0)	16.8 (14.3–20.8)	17.1 (14.2–22.2)	19.3 (13.5–23.5)	17.1 (13.2–21.9)
25(OH) vitamin D (nmol/L)	42.1 (33.3–53.8)	0.147	2.47	44.0 (26.6–53.0)	39.5 (31.8–48.5)	37.4 (29.9–44.9)	42.0 (35.8–52.0)	42.8 (35.5–55.4)	48.3 (33.8–58.6)	42.8 (33.1–54.6)
Pentosidine (pmol/L)	23.0 (18.7–28.9)	**0.518****	9.49	18.4 (16.3–22.7)	21.4 (17.4–24.2)	20.9 (17.7–24.3)	27.0 (21.2–29.0)	24.1 (20.5–31.4)	**28.0 (25.1–33.0)**[a]	**29.1 (27.5–32.8)**[a]

BMI: body mass index, CKD: chronic kidney disease, DM: diabetes mellitus, Exercise frequency; 0, 1–2, 3–4, 5–7 days per week.
Total hip: average aBMD of bilateral proximal femurs, Femoral neck: average aBMD of bilateral femoral necks, Lumbar spine: average aBMD of L1–4,
cCa: Corrected serum calcium, P: phosphate, TRACP-5b: tartrate-resistant acid phosphatase 5b, total P1NP: procollagen type 1 N-terminal propeptide, 25(OH) vitamin D: 25-hydroxyvitamin D.
Data are presented as median (interquartile range).
Spearman's rank-correlation coefficient with age, *: p<0.01, **: p<0.001 (bold).
Multiple comparison test with Bonferroni's correction, a: $p < 0.01$ compared to 20′, b: 30′, c: 40′, d: 50′, e: 60′, f: 70′, underline: $p < 0.001$ (bold).

early diagnosis and appropriate treatment are thus considered important [3–6].

Measurements of areal bone mineral density (aBMD) with dual-energy X-ray absorptiometry (DXA) are widely used in evaluating osteoporosis. Although bone fragility is strongly associated with the microstructure of cortical and trabecular bone, it cannot be evaluated by DXA. Evaluation of the bone microstructure inside the living human body has required bone biopsy of the ilium so far [7].

High-resolution peripheral quantitative computed tomography (HR-pQCT) was developed in 2004, with a voxel size of 82 μm, making it possible to evaluate bone microstructure in vivo. Since then, many studies of changes in bone microstructure due to aging, sex differences, and various diseases have been conducted [8–10]. Second-generation HR-pQCT was developed in 2014 and has an improved voxel size of 61 μm. Although some parameters were measured by indirect methods in first-generation HR-pQCT, direct measurement of bone microstructure became possible in the second generation, enabling more detailed analysis of bone microstructure [11–13].

Several previously reported studies investigated the age-related changes in bone microstructure in men with HR-pQCT, but nearly all of them used first-generation HR-pQCT [14–17]. A few studies have used second-generation HR-pQCT [18,19], but they have not examined the structure model index (SMI), connectivity density (Conn.D), degree of anisotropy (DA), and star volume of marrow space (V*ms), which are unique parameters evaluating trabecular structure three-dimensionally and have been used in various studies using micro-CT and HR-pQCT [20,21]. It may be meaningful to analyze these parameters to know more about the etiology of the age-related changes in bone microstructure in men.

In addition, relationships of bone microstructure with aBMD on DXA and bone-related biochemical markers such as tartrate-resistant acid phosphatase-5b (TRACP-5b), type I procollagen-N-propeptide (P1NP),

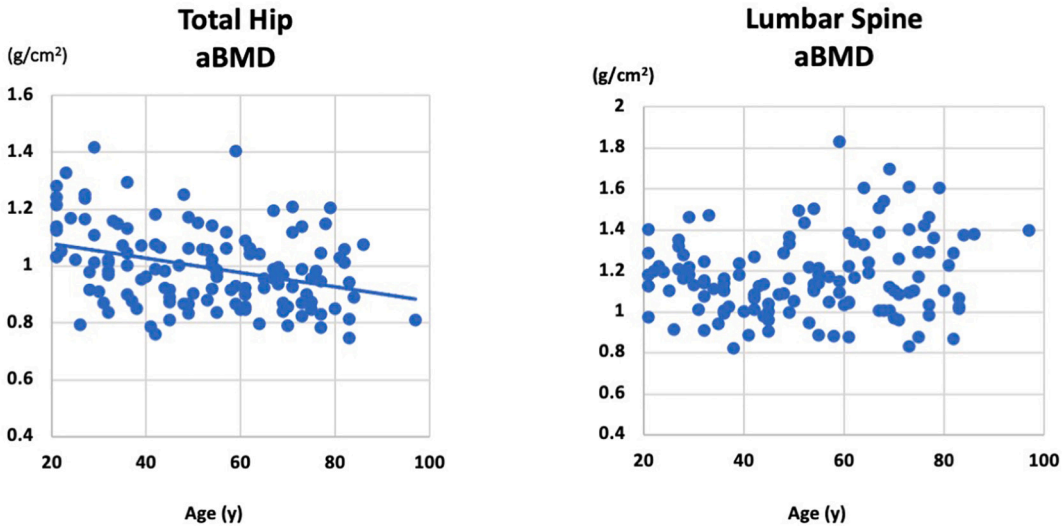

Fig. 1. Scatter plots of age and total hip and lumbar spine aBMD.

25(OH) vitamin D, and pentosidine are not well understood. By investigating bone microstructural parameters that do not correlate with aBMD, it may be possible to clarify factors related to bone fragility in men that cannot be detected by DXA. TRACP-5b is a bone resorption marker that is thought to be less susceptible to changes in renal function and diurnal variation than C-terminal telopeptide (CTX) or N-terminal telopeptide (NTX) [22,23]. Pentosidine is an advanced glycation end product (AGE), and it has been used as a surrogate marker of deteriorated collagen crosslinks in bone in recent years [24]. Analyzing the relationship between these biochemical markers and bone microstructure may be useful in clarifying the causes of age-related changes in bone microstructure in men.

The primary purpose of this study was to investigate the characteristics of age-related changes in bone microstructure at the distal radius and tibia on second-generation HR-pQCT, aBMD at the lumbar spine and proximal femur on DXA, and TRACP-5b, P1NP, vitamin D, and pentosidine on blood tests in men by conducting a cross-sectional analysis. The secondary purpose of this study was to analyze the relationships of bone microstructure with aBMD and biochemical markers.

2. Methods

2.1. Participants

The subjects were 128 healthy male volunteers who participated in a cohort study conducted in Nagasaki Prefecture, Japan (Japanese study of bone miCrostructure and minerAl density in a noRmAtive cohorT measured by HR-pQCT: J-Carat Study).

The inclusion criteria were men and 20 years of age or older, and the exclusion criteria were a history of clinical fragility fracture in the proximal femur or vertebra (men with subclinical vertebral fractures were included), a history of any of the following conditions that cause secondary osteoporosis (steroid use, rheumatoid arthritis, paralysis due to stroke, severe renal dysfunction, or hyperparathyroidism), and use of osteoporosis drugs (men taking calcium and vitamin D were included). Men undergoing cancer treatment at the time of participation in this study were also excluded.

This study was approved by the Nagasaki University Hospital Clinical Research Ethics Committee, and consent was obtained from all study participants at the time of entry (Approval no: 15083105).

2.2. DXA

aBMD was measured in the proximal femur (total hip, femoral neck) and lumbar spine (L1–4) using DXA (Prodigy Advance, GE Lunar, Madison, WI, USA). For the proximal femur, both legs were measured, and the average value was used if there was no history of hip replacement [25]. For the lumbar spine, vertebrae that had obviously higher aBMD values compared with other vertebrae as a result of degenerative changes were excluded.

2.3. Biochemical markers

Serum calcium, phosphorus, TRACP-5b, total P1NP, 25(OH) vitamin D, and pentosidine levels were measured. Serum calcium was corrected when the serum albumin level was below 4 g/dL. The correction formula was: corrected serum calcium = serum calcium + (4 – serum albumin). TRACP-5b was measured using an enzyme immunoassay (EIA) (Osteolinks TRAP-5b, SB Bioscience Co., Ltd., Tokyo, Japan), total P1NP was measured using an electro-chemiluminescence immunoassay (ECLIA) (Elecsys Total P1NP, Roche Diagnostics K.Ks., Tokyo, Japan), 25(OH) vitamin D was measured using a chemiluminescent immunoassay (CLIA) (LIAISON 25 OH Vitamin D TOTAL, Hitachi Chemical Diagnostics Systems Co., Ltd., Tokyo, Japan), and pentosidine was measured using high-performance liquid chromatography (HPLC) with a self-prepared reagent. The above tests were performed by a clinical testing company (LSI Medience Corporation, Tokyo, Japan).

2.4. HR-pQCT

Using second-generation HR-pQCT (XtreamCT II, Scanco Medical, Brittisellen, Switzerland), the non-dominant distal radius and tibia were scanned with a relative offset method [21,26,27]. For the radius, scans were centered at a position 4% of the forearm length proximal from the ulnar side of the distal articular surface of the radius. For the tibia, the scans were centered at a position 7.3% of the lower leg length proximal from the distal articular surface of the tibia. The scan conditions were as follows: tube voltage 68 kVp, tube current 1460 μA, integration time 43 ms, number of projections 900, field of view 140 mm, matrix 2304 × 2304, voxel size 60.7 μm, and total number of slices 168. Scanning time was 2 min, and the effective dose was 5 μSv. Motion artifacts were evaluated on all images, and those of grade 3 or higher were excluded [28,29].

Segmentation of the trabecular and cortical bones was performed, and the following parameters were measured on the obtained images (TRI/3D-BON, Ratoc System Engineering Co., Ltd., Tokyo, Japan) [30].

Contours of periosteal and endocortical lines were semi-automatically determined using the global threshold value of 450 mg/

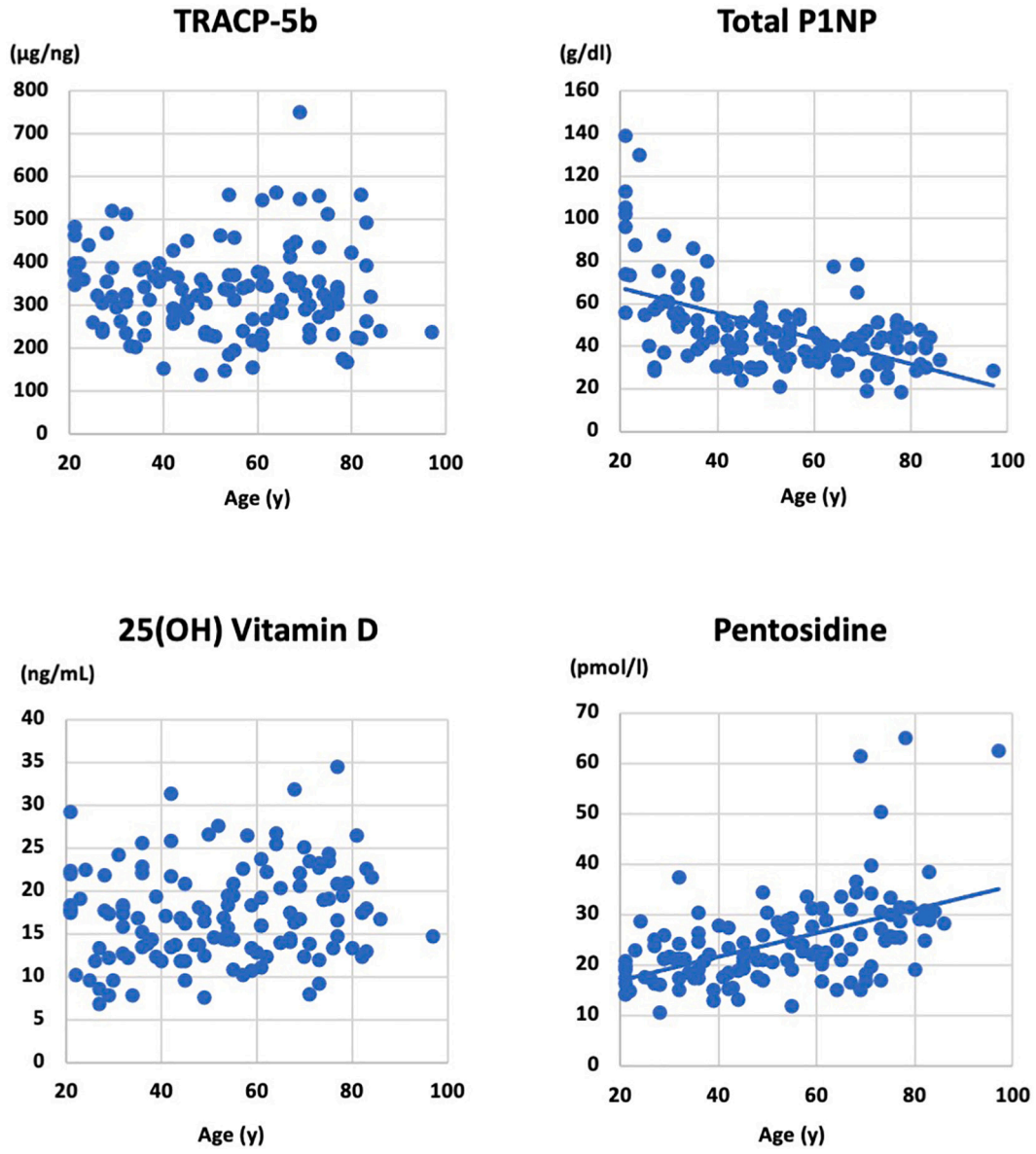

Fig. 2. Scatter plots of age and TRACP-5b, total P1NP, 25(OH) vitamin D, and pentosidine levels.

cm^3 for cortical bone adopted by the second-generation HR-pQCT [21]. In rare cases, lines were corrected manually.

Trabecular volumetric bone mineral density (Tb.vBMD), trabecular bone volume fraction (Tb.BV/TV), trabecular number (Tb.N), trabecular thickness (Tb.Th), trabecular separation (Tb.Sp), SMI, Conn.D, DA, and V*ms were measured as trabecular bone parameters.

Cortical volumetric bone mineral density (Ct.vBMD), cortical porosity (Ct.Po), cortical thickness (Ct.Th), cortical area (Ct.Ar), periosteal perimeter (Ct.Pm), and endocortical perimeter (Ec.Pm) were measured as cortical bone parameters.

BMD values were calculated from X-ray attenuation values using a regression line obtained with phantom imaging. For Tb.BV/TV and Ct.Po, the threshold values for trabecular bone and cortical bone were taken to be 320 and 450 mg/cm^3, respectively [21], and the volume density was calculated. Tb.Th, Tb.Sp, and Ct.Th were measured by the distance transformation method [21,31].

SMI expresses the three-dimensional structure of trabecular bone. A rod-like structure is taken to be 0, and a plate-like structure to be 3, and the state of the two is expressed numerically [32]. Conn.D is an indicator that evaluates the connectivity of trabecular bone. It is evaluated by the number of ring-like structures formed by trabecular bone. Higher numbers indicate higher connectivity [33]. DA is an indicator that evaluates the directionality of trabecular bone, calculated from the long and short axes of the ellipse created from the mean intercept length (MIL). Larger numbers show that the directionality of trabecular bone is large [34]. V*ms is an indicator that evaluates the cavitation of trabecular bone. By measuring lines extending radially in all directions from an arbitrary point in the bone marrow until trabeculae are touched, the cavitation of trabecular bone is evaluated. Higher values indicate higher cavitation of trabecular bone [35].

2.5. Statistical analysis

The correlations between age and DXA, biochemical markers, and HR-pQCT measurements were tested using Spearman's rank correlation coefficient. Scatter plots were created for age and each measured value, and the slopes of regression lines were obtained. The mean percentage change of measured values over 10 years was also estimated by the following formula: slope of regression line × 10/mean value for each parameter × 100. Differences between age groups (20–29, 30–39,

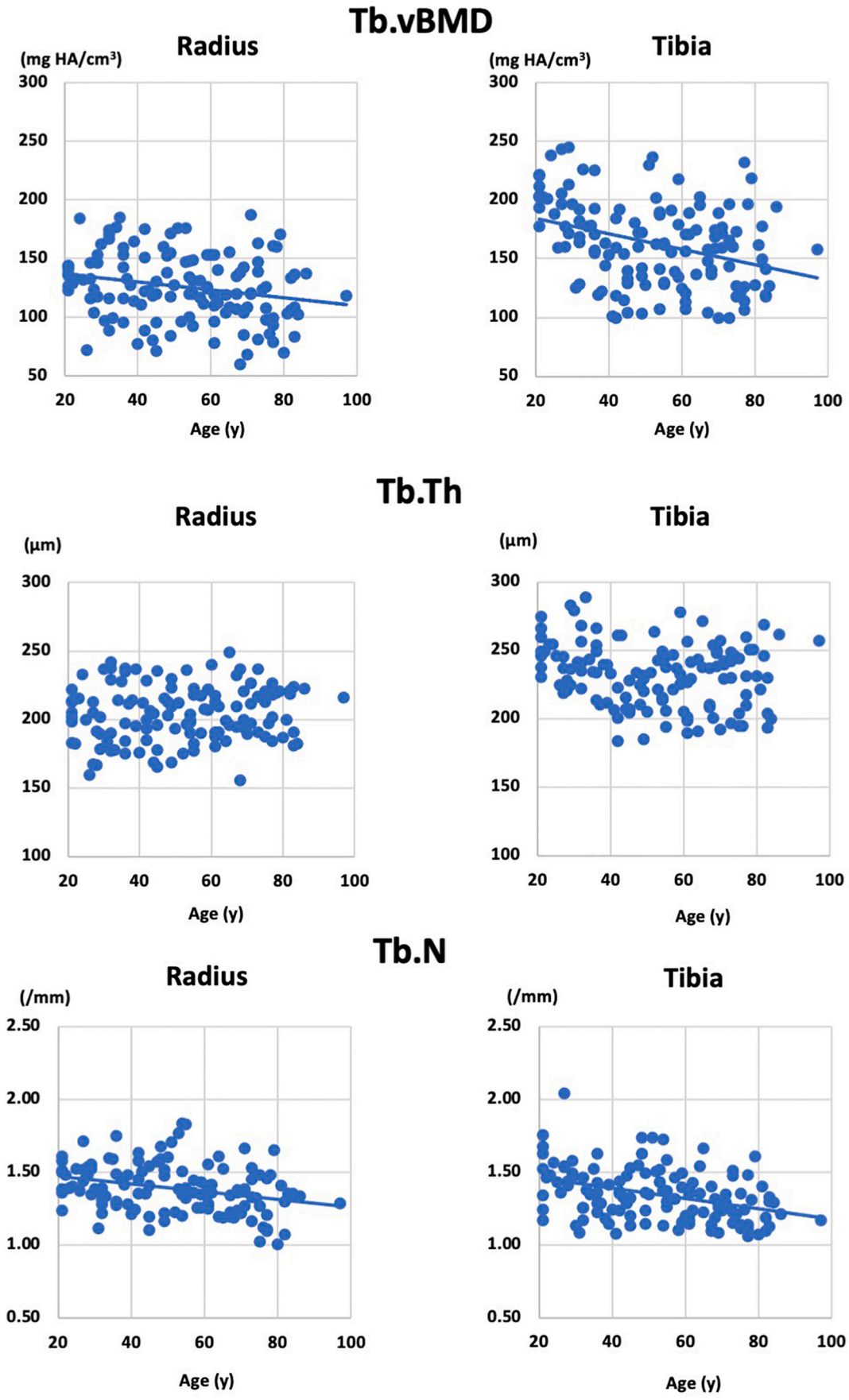

Fig. 3. Scatter plots of age and trabecular bone microstructural parameters at the distal radius and tibia.

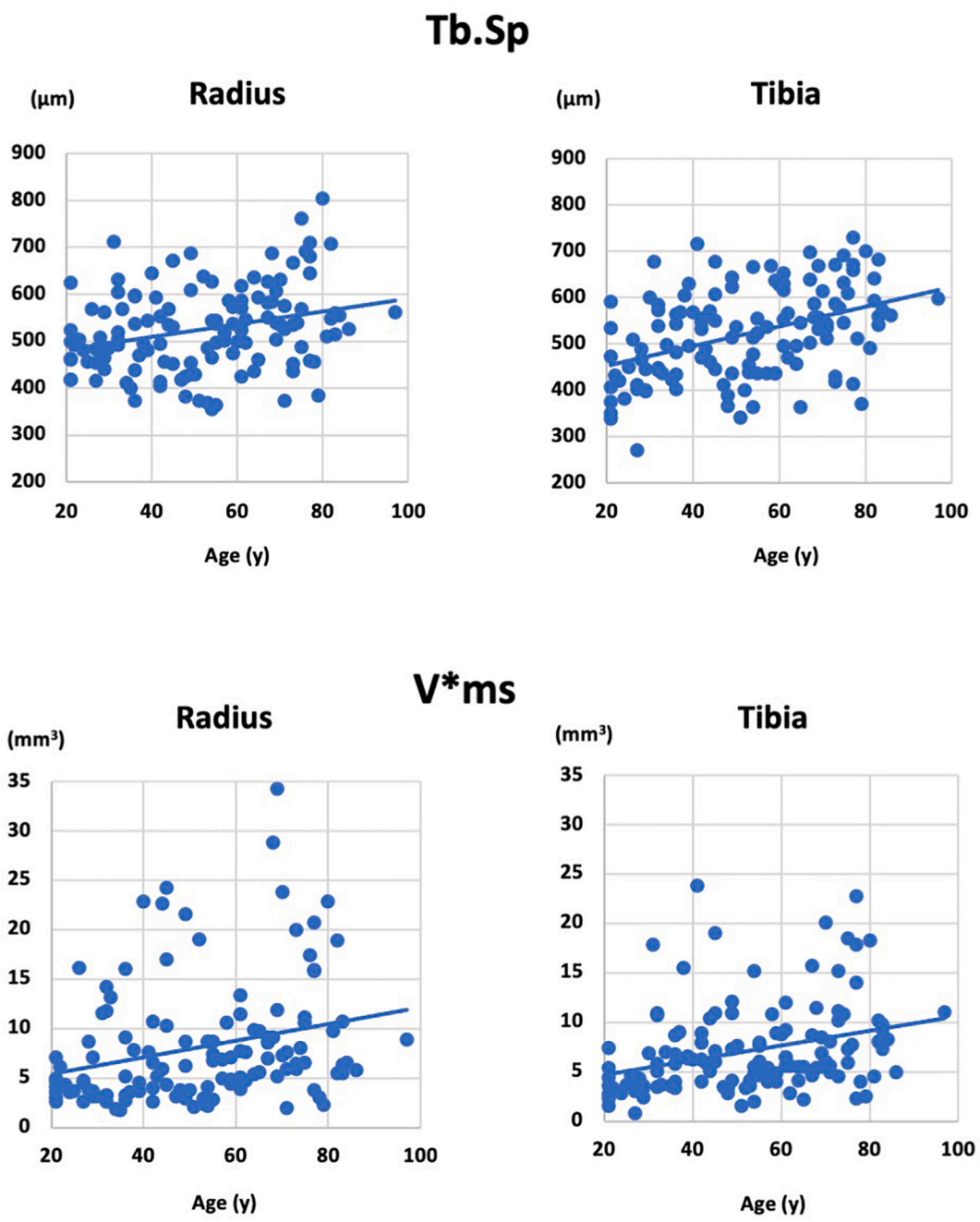

Fig. 3. (*continued*).

40–49, 50–59, 60–69, 70–79, ≥80 years) were compared using a multiple comparison test with Bonferroni's correction.

Correlations between DXA parameters, biochemical markers, and HR-pQCT parameters were tested using partial correlation coefficients adjusted for age, height, and weight.

In all tests, $P < 0.01$ was taken to indicate a significant difference (SPSS Ver. 22, IBM Corp., Armonk, NY).

3. Results

3.1. Participants

As shown in Table 1, the study participants had a median age of 53.5 years (20–97 years), median height of 169 cm (151–185 cm), median weight of 65.5 kg (48–98 kg), and median body mass index of 23.3 kg/m^2 (17.5–33.9 kg/m^2). Height and weight were significantly lower in older men.

There were 27 men with stage-3 chronic kidney disease (CKD) (eGFR 30–59 mL/min/1.73 m^2) and 0 with stage-4 CKD (eGFR <30 mL/min/1.73 m^2); 8 had type 2 diabetes mellitus, 2 with no medication, 6 with oral medication, and 0 with insulin. There was one man taking vitamin D, and no men taking calcium or osteoporosis drugs.

3.2. DXA

As shown in Table 1, Fig. 1, and Sup. Fig. 1, total hip and femoral neck aBMD were significantly lower with increased age, but no correlation was seen between lumbar spine aBMD and age. As shown in Table 1, there were 48 men with osteopenia (T-score < −1: 40 in total hip, 48 in the femoral neck, and 13 in the lumbar spine) and 5 men with

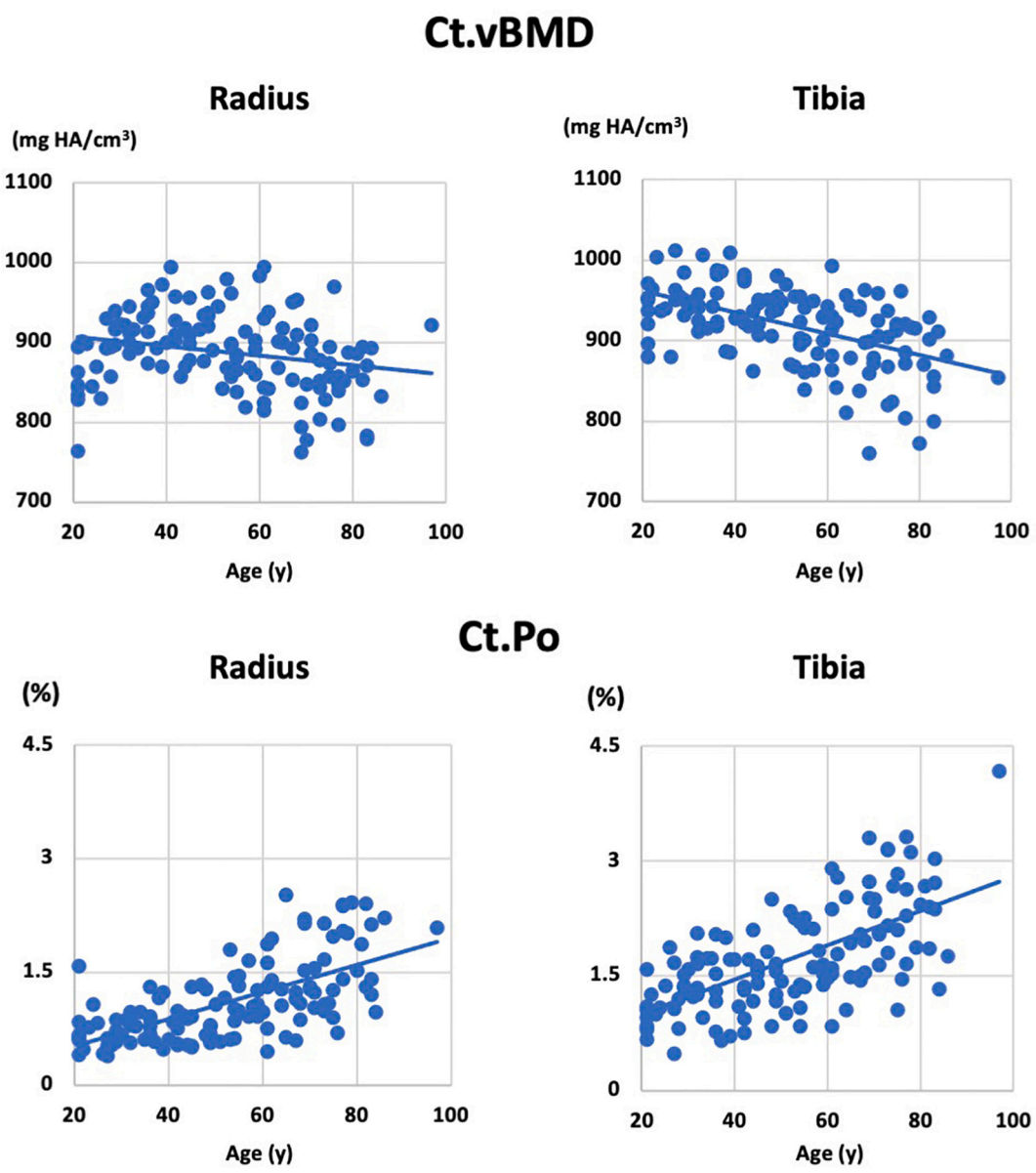

Fig. 4. Scatter plots of age and cortical bone microstructural parameters at the distal radius and tibia.

osteoporosis (T-score ≤ -2.5: 0 in total hip, 5 in the femoral neck, and 0 in the lumbar spine).

3.3. Biochemical markers

As shown in Table 1, serum calcium and phosphorus were lower in older men. As shown in Fig. 2, TRACP-5b was not significantly correlated with age, and total P1NP was negatively correlated with age, in particular being significantly higher in men in their 20s. 25(OH) vitamin D was low (median 16.9 ng/mL) regardless of age, deficient (<20 ng/mL) in 69.5% (89/128), insufficient (20–30 ng/mL) in 28.1% (36/128), and sufficient (>30 ng/mL) in 2.3% (3/128) of participants. Pentosidine was higher with increased age.

3.4. HR-pQCT

In this study, motion artifact grade 1 and 2 images were obtained in all participants, so both the distal radius and tibia were analyzed in 128 cases.

As shown in Tables 2 and 3, Figs. 3 and 5, and Sup. Fig. 2, in trabecular bone, Tb.vBMD and Tb.N were lower, and Tb.Sp was higher in both the radius and tibia of older men. V*ms was higher in older men, indicating that cavitation of the trabecular structure occurs with age. DA was lower, meaning the directionality of trabeculae decreased with increased age.

As shown in Tables 2 and 3, Figs. 4 and 5, and Sup. Fig. 3, in cortical bone, Ct.vBMD was lower, and Ct.Po was higher in both the radius and tibia in older men. Ct.Po showed the strongest correlation with age. In the tibia, Ct.Th and Ct.Ar were lower with increased age. In the radius, in contrast, a significant decrease in Ct.Ar was not seen, but Ct.Pm and Ec.Pm were significantly higher in older men.

As shown in Fig. 6, when the rate of change (%) per 10 years in bone microstructure was compared in terms of the parameters, large rates of change were seen in V*ms (10.5, 10.6%/10 years) in trabecular bone and in Ct.Po (16.2, 12.9%/10 years) in cortical bone.

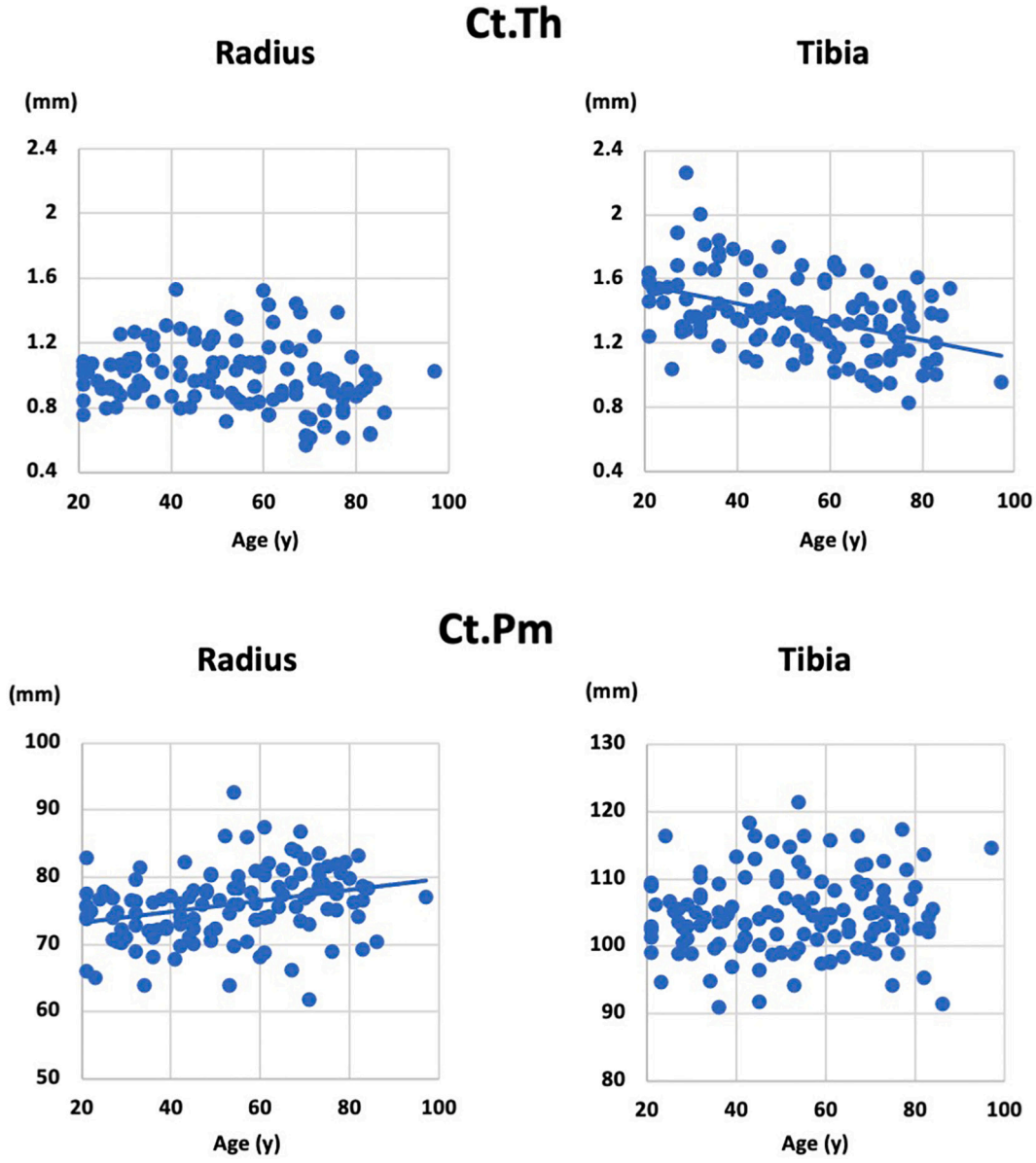

Fig. 4. (*continued*).

3.5. Correlations between DXA and HR-pQCT

As shown in Table 4, the total hip and femoral neck DXA parameters were correlated with Tb.vBMD, Tb.BV/TV, and SMI in trabecular bone in the radius, but no correlations were seen in cortical bone in the radius. In the tibia, correlations were seen with Tb.vBMD, Tb.BV/TV, Tb.Th, Tb.Sp, SMI, and V*ms in trabecular bone and Ct.vBMD, Ct.Th, and Ct.Ar in cortical bone.

In the lumbar spine, no strong correlations were seen with the radius, whereas in the tibia, correlations were seen with Tb.vBMD, Tb.BV/TV, Tb.Th, Tb.Sp, and SMI in trabecular bone and with Ct.Th and Ct.Ar in cortical bone.

In summary, the correlations between DXA and HR-pQCT parameters were stronger in the femur than in the lumbar spine, and in the tibia than in the radius.

3.6. Correlations between biochemical markers and HR-pQCT

As shown in Table 5, significant negative correlations were seen between total P1NP and Ct.vBMD of the radius and between TRACP-5b and Ct.vBMD of the tibia, but other than that, there were almost no significant correlations between TRACP-5b, P1NP, 25(OH) vitamin D, and pentosidine and bone microstructure parameters.

4. Discussion

This cross-sectional study investigated the characteristics of age-related changes in aBMD, biochemical markers, and bone microstructure, in healthy men, from young adults to seniors, using DXA, blood biochemical tests, and second-generation HR-pQCT. The relationships of aBMD and biochemical markers with bone microstructure were also analyzed.

4.1. Age-related changes in DXA parameters and biochemical markers

It has been reported that degenerative changes of the spine affect lumbar aBMD more in men than in women, and lumbar aBMD in men does not decrease even in the elderly [36]. Therefore, it is recommended that aBMD of the proximal femurs should be used to evaluate osteoporosis in men [37]. The present study also showed there was no age-

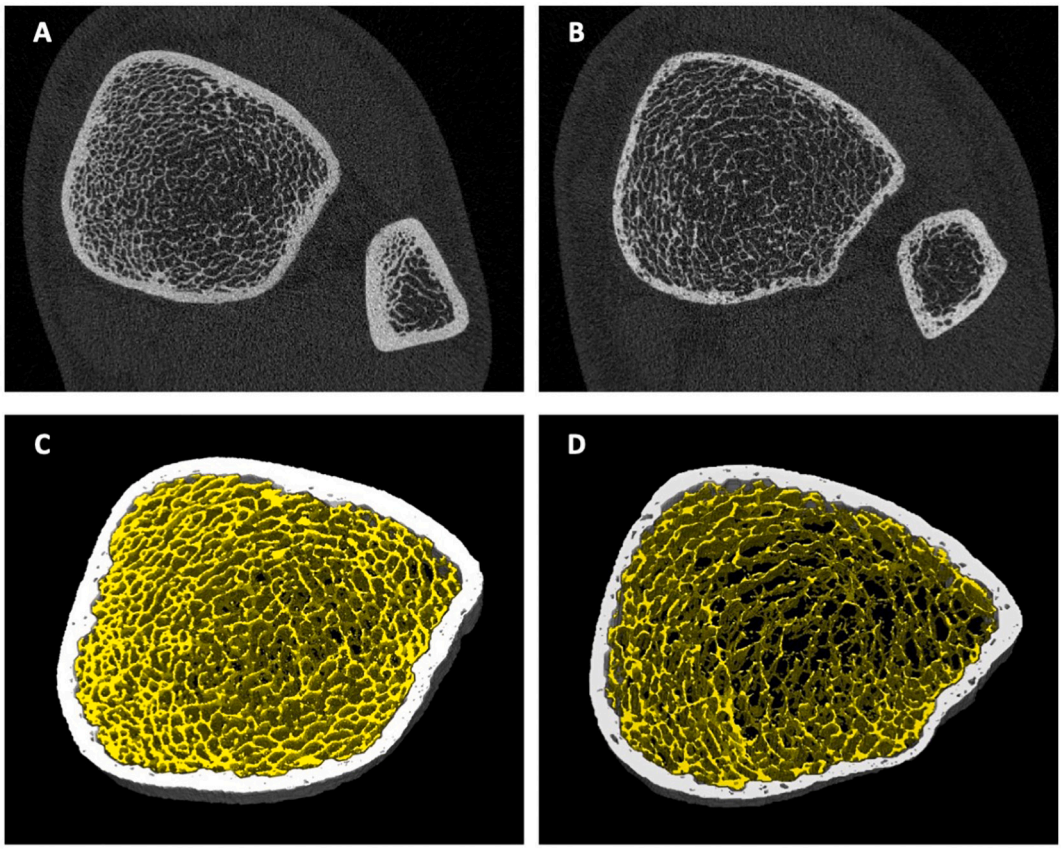

Fig. 5. Two- and three-dimensional HR-pQCT images of the distal tibia of a 21-year-old man (A and C) and a 75-year-old man (B and D). The older man shows less trabecular bone (Tb.N: 0.80 vs. 0.62, Tb.Sp: 472 vs. 691, V*ms: 4.3% vs. 18.4%) and cortical porosity (Ct.Po: 1.1% vs. 2.8%).

related decrease in the lumbar spine and a significant age-related decrease in the proximal femurs.

Previous studies reported that the bone formation marker P1NP decreases with age [38]. The high levels of P1NP in the 20s in the present study suggest the possibility that bone formation is still increased in young adult men.

Several past studies have reported that Japanese people are deficient in vitamin D, and the diet, lifestyle, and living environment are thought to be likely causes [39–42].

It has been reported that bone collagen crosslinks deteriorate with increased AGEs, which is caused by aging, chronic kidney disease, and type 2 diabetes mellitus [24]. The higher pentosidine in older men in the present study may indicate that age-related deterioration occurs not only in bone microstructure, but in also bone collagen crosslinks.

4.2. Age-related changes in HR-pQCT parameters

In trabecular bone, decreased Tb.vBMD with age was thought to be caused by a loss of trabecular bone (decreased Tb.N). Although men do not have major events that increase bone resorption such as menopause in women, trabecular bones may be gradually absorbed with aging to maintain calcium balance. Loss of trabecular bone results in cavitation of the trabecular structure (increased Tb.Sp and V*ms). Among trabecular bone parameters, V*ms, which shows cavitation of the trabecular structure, has the highest rate of change and so may be the most sensitive parameter to evaluate age-related changes in trabecular bone in men.

Previous studies using micro-CT with bone specimens from the ilium, vertebral body, and femoral neck showed that decreases in Tb.Th and Tb.N and increases in Tb.Sp occur with age in men [43,44]. In the present study, a decrease in Tb.Th was not seen. Although the resolution of the in vivo analysis with the second-generation HR-pQCT is improved compared to that of the first-generation, it is still lower than that of ex vivo analysis by micro-CT. It is considered that different results from micro-CT were obtained because thin trabecular bones less than 100 μm are not adequately captured with HR-pQCT.

In cortical bone, decreased Ct.vBMD and increased Ct.Po with age were thought to occur by bone resorption in cortical bone to maintain calcium metabolism, as well as trabecular bone. Ct.Po showed the greatest rate of change among cortical bone parameters, and it is thought to be the most sensitive parameter to evaluate the age-related changes in cortical bone.

Decreased Ct.Th with age in the tibia might occur because the tibia is a weight-bearing bone and is more affected by the activity level. In contrast, larger Ct.Pm with age in the radius might be a compensatory response to maintain bone strength with the larger diameter.

Hansen et al. evaluated bone microstructure in adult Danish men and women using first-generation HR-pQCT and reported that, in men, Tb.vBMD and Tb.Th decreased and Ct.Po increased with age, but no changes were seen in Ct.Th [15]. Zhu et al. analyzed bone microstructure in adult Chinese men and women using first-generation HR-pQCT, and they reported that, in men, Tb.vBMD and Ct.vBMD decreased gradually with age, although the timing of the start of those decreases differed, whereas Ct.Po increased, and Ct.Th was maintained [17]. With first-generation and second-generation HR-pQCT, not only the resolution, but also the analytical algorithm differs, which may have contributed to the differing results [21].

Yu et al. analyzed bone microstructure in adult Chinese men and women using second-generation HR-pQCT, and reported that Tb.vBMD, Tb.N, and Tb.Th decreased with age, Tb.Sp increased, Ct.Th decreased, and Ct.Po showed the highest rate of increase in men [18]. This suggests that the trends in age-related changes in bone microstructure are similar

Table 2
Measurement values of HR-pQCT parameters at the distal radius and their correlations with age, change (%) over 10 years, and comparisons among generations.

Distal Radius	Total	Correlation with age	Change (%) in 10 years	Age (20–29 y)	(30–39 y)	(40–49 y)	(50–59 y)	(60–69 y)	(70–79 y)	(≥80 y)
Trabecular bone										
Tb.vBMD (mg HA/cm^3)	124 (105–147)	**−0.228****	−2.70	133 (123–144)	142 (114–167)	121 (90.5–152)	128 (117–148)	116 (104–140)	120 (94.3–157)	108 (100–134)
Tb.BV/TV (%)	21.6 (18.0–25.5)	−0.177*	−1.86	23.6 (18.4–25.9)	25.4 (16.8–28.3)	21.6 (14.7–26.2)	22.7 (21.0–25.9)	20.5 (18.5–24.2)	21.3 (16.5–26.6)	19.3 (17.6–23.0)
Tb.Th (μm)	204 (190–219)	0.109	0.55	200 (183–213)	214 (184–237)	204 (179–215)	204 (190–218)	200 (190–220)	214 (196–220)	208 (186–222)
Tb.N (/mm)	1.37 (1.27–1.50)	**−0.360****	−1.59	1.49 (1.39–1.53)	1.35 (1.28–1.48)	1.43 (1.23–1.57)	1.39 (1.33–1.61)	1.31 (1.22–1.40)	1.33 (1.18–1.47)	1.33 (1.23–1.36)
Tb.Sp (μm)	527 (459–584)	**0.288****	2.56	473 (454–508)	503 (471–595)	513 (427–604)	502 (430–544)	560 (500–604)	538 (457–661)	557 (524–598)
SMI	1.69 (1.49–1.87)	0.218*	2.26	1.53 (1.27–1.75)	1.67 (1.15–1.88)	1.75 (1.50–2.08)	1.64 (1.52–1.83)	1.70 (1.65–1.87)	1.73 (1.50–1.86)	1.82 (1.67–2.05)
Conn.D (/mm^3)	3.22 (2.67–4.02)	**−0.231****	−3.20	3.86 (3.21–4.34)	3.12 (2.66–3.63)	3.33 (2.31–4.11)	3.49 (2.91–4.37)	2.94 (2.46–3.76)	2.89 (2.26–3.66)	2.92 (2.51–3.25)
DA	1.91 (1.80–2.04)	**−0.242****	−1.10	2.00 (1.90–2.17)	1.94 (1.83–2.08)	1.91 (1.80–2.05)	1.85 (1.72–2.17)	1.89 (1.76–2.02)	1.85 (1.81–2.00)	1.81 (1.78–1.95)
V*ms (mm^3)	6.22 (3.77–9.84)	**0.340****	10.45	4.20 (3.56–5.87)	3.71 (3.19–11.6)	6.41 (3.85–15.5)	4.95 (2.97–8.65)	8.14 (5.26–11.1)	7.46 (5.91–16.0)	7.76 (5.78–12.8)
Cortical bone										
Ct.vBMD (mg HA/cm^3)	893 (854–920)	**−0.251****	−0.66	881 (844–899)	917 (894–945)	917 (898–937)	885 (860–902)	897 (829–936)	**855 (840–887)**[bc]	868 (820–893)
Ct.Po (%)	0.97 (0.67–1.32)	**0.665****	16.24	0.62 (0.53–0.81)	0.87 (0.66–0.97)	0.77 (0.55–0.92)	1.05 (0.92–1.32)	**1.26 (0.9–1.8)**[abc]	**1.36 (1.07–2.04)**[abc]	**1.70 (1.28–2,15)**[abcd]
Ct.Th (mm)	0.96 (0.85–1.09)	−0.210*	−1.98	0.94 (0.88–1.06)	1.10 (0.94–1.25)	1.00 (0.88–1.29)	0.93 (0.84–1.08)	0.92 (0.76–1.29)	0.90 (0.77–0.98)	0.91 (0.74–1.00)
Ct.Ar (mm^2)	66.6 (59.3–76.7)	−0.129	−1.20	64.1 (58.4–70.2)	72.9 (63.9–77.4)	67.6 (62.5–82.0)	65.4 (59.4–78.0)	64.8 (57.4–87.4)	65.1 (55.4–68.7)	63.0 (48.5–68.9)
Ct.Pm (mm)	76.1 (72.3–79.0)	**0.345****	1.06	74.5 (71.1–76.9)	72.4 (71.1–76.5)	75.1 (71.3–77.9)	76.5 (73.6–80.2)	78.9 (74.0–81.8)	78.5 (75.7–81.5)	76.8 (73.2–79.0)
Ec.Pm (mm)	71.6 (66.8–75.1)	**0.357****	1.28	70.5 (66.4–72.6)	67.3 (65.4–71.5)	71.0 (66.8–73.1)	72.2 (69.9–75.9)	75.4 (67.4–78.1)	74.7 (71.7–77.6)	73.0 (68.5–75.0)

Tb.vBMD: trabecular volumetric bone mineral density, Tb.BV/TV: bone volume fraction, Tb.Th: trabecular thickness, Tb.N: trabecular number, Tb.Sp: trabecular separation, SMI: structure model index, Conn.D: connectivity density, DA: Degree of anisotropy, V*ms: star volume of marrow space, Ct.vBMD: cortical volumetric bone mineral density, Ct.Po: cortical porosity, Ct.Th: cortical thickness, Ct.Ar: cortical area, Ct.Pm: periosteal perimeter, Ec.Pm: endocortical perimeter.
Data are presented as median (interquartile range).
Spearman's rank-correlation coefficient with age, *: p<0.01, **: p<0.001 (bold).
Multiple comparison test with Bonferroni's correction, a: $p < 0.01$ compared to 20′, b: 30′, c: 40′, d: 50′, e: 60′, f: 70′, underline: $p < 0.001$ (bold).

between Japanese and Chinese persons in East Asia. Whittier et al. investigated bone microstructure in adult Canadian men and women using second-generation HR-pQCT, and they reported that Tb.vBMD, Tb.N, and Tb.Th decreased with age, Tb.Sp increased, Ct.vBMD and Ct.Th decreased, and Ct.Po increased in men [19]. This means that, even if there is a certain degree of difference among races in terms of physiques, genetic factors, nutrition, and daylight hours, the age-related changes in bone microstructure have something in common.

4.3. Relationships between DXA and HR-pQCT parameters

Stronger correlations between DXA at the proximal femur and HR-pQCT at the distal tibia may be because both of them are weight-bearing bones of the legs. Another possible cause is that the lumbar spine may not have been accurately evaluated in some of the cases because of the effects of degenerative changes. In order to attempt to reduce the effects of degenerative changes on DXA at the lumbar spine, vertebral bodies with obvious higher aBMD due to osteophytes, scoliosis, and so on were excluded, but it was impossible to exclude them completely. Amstrup et al. compared DXA and HR-pQCT parameters in postmenopausal women and found that aBMD of the proximal femur was more strongly correlated with HR-pQCT parameters than aBMD of the lumbar spine, similar to the present study [45].

On the other hand, Ct.Po, which had the greatest age-related change among all HR-pQCT parameters in the present study, had no correlation with DXA parameters, meaning that osteoporosis and fracture risk caused by Ct.Po may be overlooked in standard clinical medicine.

4.4. Relationships between biochemical markers and HR-pQCT parameters

Chaitou et al. examined the relationship between bone turnover markers and bone microstructure measured with first-generation HR-pQCT, and, similar to the present study, they found that CTX, osteocalcin (OC), and P1NP were negatively correlated with Ct.vBMD [14]. Increased bone resorption creates cortical porosity, and increased bone formation produces low calcified bone tissue; thus, both of them are thought to decrease Ct.vBMD.

Boyd et al. reported that correlations between serum 25(OH) vitamin D and HR-pQCT parameters were not strong [46], and the present study found the same. There were no reports analyzing the relationship between pentosidine and HR-pQCT parameters.

4.5. Limitations

There were several limitations in this study. First, the research

Table 3
Measurement values of HR-pQCT parameters at the distal tibia and their correlations with age, change (%) over 10 years, and comparisons among generations.

Distal tibia	Total	Correlation with age	Change (%) in 10 years	Age (20–29 y)	(30–39 y)	(40–49 y)	(50–59 y)	(60–69 y)	(70–79 y)	(≥80 y)
Trabecular bone										
Tb.vBMD (mg HA/cm^3)	162 (131–191)	**−0.351****	−4.05	202 (180–218)	169 (144–192)	**141 (116–169)**[a]	162 (135–191)	**157 (128–173)**[a]	**160 (119–186)**[a]	**146 (125–166)**[a]
Tb.BV/TV (%)	26.7 (22.2–30.0)	**−0.384****	−4.05	32.3 (29.5–35.1)	26.9 (24.6–29.6)[a]	**23.7 (20.3–28.4)**[a]	26.6 (22.6–31.2)	**25.3 (21.3–28.1)**[a]	**25.8 (19.4–29.2)**[a]	**23.7 (20.9–26.8)**[a]
Tb.Th (μm)	234 (214–248)	−0.183*	−1.06	246 (229–254)	241 (233–257)	218 (207–231) [a]	232 (215–246)	233 (202–247)	235 (205–248)	231 (203–258)
Tb.N (/mm)	1.34 (1.21–1.47)	**−0.331****	−2.31	1.49 (1.42–1.58)	1.29 (1.19–1.43)[a]	1.34 (1.24–1.49)	1.38 (1.30–1.51)	**1.25 (1.18–1.38)**[a]	**1.26 (1.14–1.35)**[a]	**1.20 (1.12–1.31)**[a]
Tb.Sp (μm)	532 (438–593)	**0.414****	4.07	417 (386–470)	538 (443–585)	538 (450–597)[a]	478 (436–536)	**557 (497–629)**[a]	**561 (512–652)**[a]	**583 (555–652)**[a]
SMI	1.36 (1.14–1.62)	0.237*	3.26	1.10 (0.78–1.18)	1.38 (1.14–1.68)[a]	**1.62 (1.40–1.76)**[a]	1.33 (1.18–1.57)[a]	1.33 (1.17–1.56)[a]	**1.41 (1.14–1.69)**[a]	1.44 (1.27–1.68)[a]
Conn.D (/mm^3)	3.78 (3.00–4.54)	−0.148	−2.38	3.90 (3.46–4.82)	3.24 (2.54–4.19)	4.14 (3.20–4.60)	3.99 (3.48–5.45)	3.64 (3.00–4.82)	3.41 (2.75–3.92)	3.14 (2.35–4.27)
DA	2.00 (1.91–2.09)	**−0.307****	−1.05	2.06 (1.96–2.12)	2.10 (1.97–2.15)	1.97 (1.90–2.09)	1.99 (1.87–2.05)	1.98 (1.93–2.05)	1.95 (1.88–2.06)	1.97 (1.84–2.05)
V*ms (mm^3)	5.83 (2.75–8.77)	**0.381****	10.59	3.31 (2.69–4.14)	6.47 (3.86–8.89)	6.57 (4.30–10.7)[a]	4.71 (3.91–7.58)	5.92 (5.33–8.68)	**7.78 (5.03–14.8)**[a]	8.67 (6.60–10.3)
Cortical bone										
Ct.vBMD (mg HA/cm^3)	924 (886–951)	**−0.516****	−1.44	951 (933–963)	942 (917–982)	937 (921–969)	903 (870–947)	907 (861–943)[a]	909 (872–921)[ab]	**863 (832–904)**[abc]
Ct.Po (%)	1.63 (1.27–2.13)	**0.623****	12.93	1.10 (0.87–1.38)	1.54 (1.18–1.74)	1.47 (1.18–1.70)	1.62 (1.37–2.17)	**1.86 (1.50–2.53)**[a]	**2.23 (1.82–2.80)**[abcd]	**2.42 (1.84–2.80)**[abcd]
Ct.Th (mm)	1.36 (1.21–1.54)	**−0.402****	−4.26	1.53 (1.28–1.62)	1.44 (1.35–1.76)	1.40 (1.26–1.52)	1.32 (1.25–1.39)	1.32 (1.09–1.46)	1.26 (1.09–1.40)[ab]	1.14 (1.00–1.41)[b]
Ct.Ar (mm^2)	135 (120–153)	**−0.427****	−3.86	151 (128–156)	141 (127–165)	137 (128–156)	132 (119–142)	123 (111–143)	121 (108–137)[ab]	111 (102–132)[ab]
Ct.Pm (mm)	105 (101–109)	0.040	0.16	103 (101–107)	104 (99.7–107)	104 (100–112)	106 (99.8–111)	105 (100–110)	104 (102–107)	104 (100–110)
Ec.Pm (mm)	98.8 (95.1–104)	0.155	0.52	(94.9–101)	97.9 (92.4–101)	98.2 (94.2–108)	100 (95.1–106)	101 (94.7–106)	99.6 (97.5–102)	99.7 (95.4–106)

Tb.vBMD: trabecular volumetric bone mineral density, Tb.BV/TV: bone volume fraction, Tb.Th: trabecular thickness, Tb.N: trabecular number, Tb.Sp: trabecular separation, SMI: structure model index, Conn.D: connectivity density, DA: Degree of anisotropy, V*ms: star volume of marrow space, Ct.vBMD: cortical volumetric bone mineral density, Ct.Po: cortical porosity, Ct.Th: cortical thickness, Ct.Ar: cortical area, Ct.Pm: periosteal perimeter, Ec.Pm: endocortical perimeter.

Data are presented as median (interquartile range).

Spearman's rank-correlation coefficient with age, *: p<0.01, **: p<0.001 (bold).

Multiple comparison test with Bonferroni's correction, a: $p < 0.01$ compared to 20′, b: 30′, c: 40′, d: 50′, e: 60′, f: 70′, underline: $p < 0.001$ (bold).

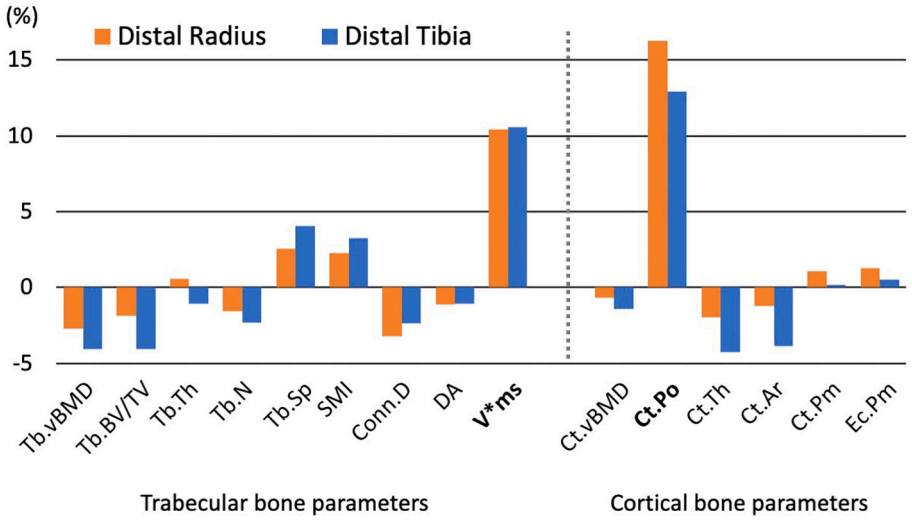

Fig. 6. Change rates over 10 years of trabecular and cortical bone microstructural parameters.

Table 4
Partial correlation coefficients between DXA and HR-pQCT parameters adjusted by age, height, and weight.

Distal radius	Total hip	Femoral neck	Lumbar spine
Trabecular			
Tb.vBMD	**0.423****	**0.419****	0.259*
Tb.BV/TV	**0.390****	**0.360****	0.213
Tb.Th	0.266*	0.296*	0.180
Tb.N	0.255*	0.153	0.108
Tb.Sp	**−0.315****	−0.225	−0.155
SMI	**−0.390****	**−0.394****	−0.233*
Conn.D	0.262*	0.171	0.131
DA	**0.310****	0.297*	0.245*
V*ms	−0.294*	−0.239*	−0.157
Cortical			
Ct.vBMD	0.116	0.129	0.170
Ct.Po	0.109	0.143	0.055
Ct.Th	0.193	0.191	0.177
Ct.Ar	0.203	0.215	0.233*
Ct.Pm	−0.057	−0.024	0.057
Ec.Pm	−0.089	−0.055	0.027

Distal tibia	Total hip	Femoral neck	Lumbar spine
Trabecular			
Tb.vBMD	**0.610****	**0.611****	**0.480****
Tb.BV/TV	**0.598****	**0.579****	**0.460****
Tb.Th	**0.444****	**0.517****	**0.351****
Tb.N	**0.354****	0.240*	0.276*
Tb.Sp	**−0.463****	**−0.367****	**−0.345****
SMI	**−0.435****	**−0.453****	**−0.323****
Conn.D	0.097	−0.028	0.033
DA	−0.006	−0.014	−0.035
V*ms	**−0.450****	**−0.370****	−0.299*
Cortical			
Ct.vBMD	**0.366****	**0.362****	0.297*
Ct.Po	−0.232*	−0.166	−0.114
Ct.Th	**0.562****	**0.554****	**0.350****
Ct.Ar	**0.609****	**0.610****	**0.412****
Ct.Pm	0.012	0.034	0.088
Ec.Pm	−0.092	−0.061	0.030

Tb.vBMD: trabecular volumetric bone mineral density, Tb.BV/TV: bone volume fraction, Tb.Th: trabecular thickness, Tb.N: trabecular number, Tb.Sp: trabecular separation, SMI: structure model index, Conn.D: connectivity density, DA: Degree of anisotropy, V*ms: star volume of marrow space, Ct.vBMD: cortical volumetric bone mineral density, Ct.Po: cortical porosity, Ct.Th: cortical thickness, Ct.Ar: cortical area, Ct.Pm: periosteal perimeter, Ec.Pm: endocortical perimeter.
Partial correlation coefficients adjusted by age, height, and weight, * $p<0.01$, ** $p<0.001$ (bold).

participants were all men, and the characteristics of age-related changes in bone microstructure in men were not compared to those in women. In addition, all subjects were racially Japanese, and differences due to race were not investigated. Moreover, although the ages of study participants were widespread and evenly distributed, the overall number of participants was small, and a large-scale study is desired in the future. This was also a cross-sectional study, and so it is not known whether these are truly age-related changes. A longitudinal study is planned for the future. Although a semi-automatic technique was used to make reproducible measurements of bone microstructure, the true endocortical surface cannot be determined accurately, and there is a possibility that cortical bone parameters were over or underestimated. Finite element analysis was not performed to estimate bone strength, such as stiffness and failure load. Blood sampling time was not taken into account; of the measured items, 25(OH) vitamin D might be affected by diet and season. Finally, levels of sex hormones, such as androgen and estrogen, were not examined in the blood tests.

5. Conclusions

Age-related changes in bone microstructure, aBMD, and biochemical markers were investigated cross-sectionally in men. Decreased Tb.vBMD with decreased Tb.N and cavitation of trabecular structure (increased Tb.Sp and V*ms) were seen in trabecular bone, and decreased Ct.vBMD with increased Ct.Po were seen in cortical bone. In particular, Ct.Po was the most strongly correlated with age of all the parameters. aBMD in the proximal femur and P1NP were lower and pentosidine was higher with age, whereas no age-related changes were seen in aBMD of the lumbar spine, TRACP-5b, and 25(OH) vitamin D levels.

For the relationships between DXA and HR-pQCT, stronger correlations were seen between aBMD of the proximal femur and bone microstructure of the tibia, whereas no DXA parameters had correlations with Ct.Po. For the relationships between blood biochemical markers and HR-pQCT, correlations were seen between elevations of bone turnover markers and decreased Ct.vBMD, but other than that, TRACP-5b, P1NP, 25(OH) vitamin D, and pentosidine were not obviously correlated with bone microstructure.

Supplementary data to this article can be found online at https://doi.org/10.1016/j.bone.2021.116252.

Declaration of competing interest

All authors have no conflict of interest.

Table 5
Partial correlation coefficients between biochemical markers and HR-pQCT parameters adjusted by age, height, and weight.

Distal radius	TRACP-5b	Total P1NP	25(OH) vitamin D	Pentosidine
Trabecular				
Tb.vBMD	0.026	0.037	−0.070	0.184
Tb.BV/TV	0.049	0.070	−0.038	0.151
Tb.Th	0.062	0.101	−0.052	0.159
Tb.N	−0.023	−0.102	0.020	0.027
Tb.Sp	0.014	0.066	0.014	−0.073
SMI	−0.090	−0.188	0.058	−0.152
Conn.D	0.032	−0.045	0.057	0.011
DA	0.083	0.077	−0.132	0.097
V*ms	0.064	0.025	0.097	0.030
Cortical				
Ct.vBMD	−0.237*	**−0.347****	−0.122	0.112
Ct.Po	0.095	0.231*	0.246*	0.089
Ct.Th	−0.142	−0.124	−0.069	0.119
Ct.Ar	−0.100	−0.074	0.013	0.140
Ct.Pm	0.155	0.164	0.236*	0.023
Ec.Pm	0.188	0.183	0.233*	0.014

Distal tibia	TRACP-5b	Total P1NP	25(OH)D	Pentosidine
Trabecular				
Tb.vBMD	0.051	0.157	−0.080	0.233*
Tb.BV/TV	0.077	0.159	−0.079	0.220
Tb.Th	0.068	0.196	−0.113	0.244*
Tb.N	0.027	−0.003	−0.006	0.045
Tb.Sp	−0.043	−0.057	0.034	−0.099
SMI	−0.084	−0.158	0.059	−0.125
Conn.D	0.062	−0.074	0.044	−0.024
DA	−0.105	−0.098	−0.228*	0.123
V*ms	−0.031	−0.024	0.034	−0.139
Cortical				
Ct.vBMD	**−0.308****	−0.281*	−0.153	0.160
Ct.Po	0.181	0.112	0.013	0.137
Ct.Th	−0.166	−0.149	−0.111	0.132
Ct.Ar	−0.129	−0.093	−0.022	0.178
Ct.Pm	0.125	0.161	0.244*	0.098
Ec.Pm	0.171	0.185	0.232*	0.080

Tb.vBMD: trabecular volumetric bone mineral density, Tb.BV/TV: bone volume fraction, Tb.Th: trabecular thickness, Tb.N: trabecular number, Tb.Sp: trabecular separation, SMI: structure model index, Conn.D: connectivity density, DA: Degree of anisotropy, V*ms: star volume of marrow space, Ct.vBMD: cortical volumetric bone mineral density, Ct.Po: cortical porosity, Ct.Th: cortical thickness, Ct.Ar: cortical area, Ct.Pm: periosteal perimeter, Ec.Pm: endocortical perimeter, TRACP-5b: tartrate-resistant acid phosphatase 5b, total P1NP: procollagen type 1 N-terminal propeptide, 25(OH) vitamin D: 25-hydroxyvitamin D.
Partial correlation coefficients adjusted by age, height, and weight, * $p<0.01$, ** $p<0.001$ (bold).

CRediT authorship contribution statement

Mitsuru Doi: Investigation, Formal analysis, Writing – original draft. **Ko Chiba:** Conceptualization, Methodology, Writing – review & editing. **Narihiro Okazaki:** Investigation, Writing – review & editing. **Choko Kondo:** Investigation, Supervision. **Shuta Yamada:** Investigation. **Kazuaki Yokota:** Investigation. **Akihiko Yonekura:** Supervision. **Masato Tomita:** Supervision. **Makoto Osaki:** Writing – review & editing, Supervision.

Acknowledgments

The authors would like to thank Mika Kono and Yasue Michikoshi for performing DXA analysis.

Funding

The study was supported by JSPS KAKENHI grant number 19K18535 and a research grant from the Japan Orthopedics and Traumatology Foundation. The funders had no involvement in the study design; the collection, analysis and interpretation of data; in the writing of the report; or in the decision to submit the article for publication.

Ethics approval

This study was approved by the Nagasaki University Hospital Clinical Research Ethical Committee (registration numbers: 15083105). The protocol was designed and conducted in accordance with the Declaration of Helsinki (1964) and its later amendments.

Consent to participate

Informed consent was obtained from all participants in this study.

References

[1] Assessment of fracture risk and its application to screening for postmenopausal osteoporosis, in: Report of a WHO Study Group, World Health Organ Tech Rep Ser. 843, 1994, pp. 1–129.
[2] NIH, Consensus Development Panel on Osteoporosis Prevention, Diagnosis, and Therapy, Osteoporosis Prevention, Diagnosis, and Therapy, JAMA (2001) 785–795.
[3] J.R. Center, T.V. Nguyen, D. Schneider, P.N. Sambrook, J.A. Eisman, Mortality after all major types of osteoporotic fracture in men and women: an observational study, Lancet 353 (1999) 878–882.
[4] D. Bliuc, N.D. Nguyen, V.E. Milch, T.V. Nguyen, J.A. Eisman, J.R. Center, Mortality risk associated with low-trauma osteoporotic fracture and subsequent fracture in men and women, JAMA 301 (2009) 513–521.
[5] M. von Friesendorff, F.E. McGuigan, J. Besjakov, K. Akesson, Hip fracture in men-survival and subsequent fractures: a cohort study with 22-year follow-up, J. Am. Geriatr. Soc. 59 (2011) 806–813.
[6] S.A. Frost, N.D. Nguyen, J.R. Center, J.A. Eisman, T.V. Nguyen, Excess mortality attributable to hip-fracture: a relative survival analysis, Bone 56 (2013) 23–29.
[7] D.W. Dempster, J.E. Compston, M.K. Drezner, F.H. Glorieux, J.A. Kanis, H. Malluche, et al., Standardized nomenclature, symbols, and units for bone histomorphometry: a 2012 update of the report of the ASBMR Histomorphometry Nomenclature Committee, J Bone Miner Res. 28 (2013) 2–17.
[8] A.J. Burghardt, T.M. Link, S. Majumdar, High-resolution computed tomography for clinical imaging of bone microarchitecture, Clin. Orthop. Relat. Res. 469 (2011) 2179–2193.
[9] A.M. Cheung, J.D. Adachi, D.A. Hanley, D.L. Kendler, K.S. Davison, R. Josse, et al., High-resolution peripheral quantitative computed tomography for the assessment of bone strength and structure: a review by the Canadian bone strength working group, Curr. Osteoporos. Rep. 11 (2013) 136–146.
[10] K.K. Nishiyama, E. Shane, Clinical imaging of bone microarchitecture with HR-pQCT, Curr. Osteoporos. Rep. 11 (2013) 147–155.
[11] S.L. Manske, Y. Zhu, C. Sandino, S.K. Boyd, Human trabecular bone microarchitecture can be assessed independently of density with second generation HR-pQCT, Bone 79 (2015) 213–221.
[12] K. Chiba, N. Okazaki, A. Kurogi, Y. Isobe, A. Yonekura, M. Tomita, et al., Precision of second-generation high-resolution peripheral quantitative computed tomography: intra- and intertester reproducibilities and factors involved in the reproducibility of cortical porosity, J. Clin. Densitom. 21 (2018) 295–302.
[13] K. Yokota, K. Chiba, N. Okazaki, C. Kondo, M. Doi, S. Yamada, et al., Deterioration of bone microstructure by aging and menopause in Japanese healthy women: analysis by HR-pQCT, journal of bone and mineral, Metabolism 38 (2020) 826–838.
[14] A. Chaitou, S. Boutroy, N. Vilayphiou, F. Munoz, P.D. Delmas, R. Chapurlat, et al., Association between bone turnover rate and bone microarchitecture in men: the STRAMBO study, J. Bone Miner. Res. 25 (2010) 2313–2323.
[15] S. Hansen, V. Shanbhogue, L. Folkestad, M.M.F. Nielsen, K. Brixen, Bone microarchitecture and estimated strength in 499 adult danish women and men: a cross-sectional, population-based high-resolution peripheral quantitative computed tomographic study on peak bone, Structure 94 (2013) 269–281.
[16] L.A. Burt, Z. Liang, T.T. Sajobi, D.A. Hanley, S.K. Boyd, Sex- and site-specific normative data curves for HR-pQCT, J. Bone Miner. Res. 31 (2016) 2041–2047.
[17] T.Y. Zhu, B.H. Yip, V.W. Hung, C.W. Choy, K.-L. Cheng, T.C. Kwok, et al., Normative standards for HRpQCT parameters in Chinese men and women, J. Bone Miner. Res. 33 (10) (2018 Oct) 1889–1899.
[18] F. Yu, Y. Xu, Y. Hou, Y. Lin, R. Jiajue, Y. Jiang, et al., Age-, site-, and sex-specific normative centile curves for HR-pQCT-derived microarchitectural and bone strength parameters in a Chinese mainland population, J. Bone Miner. Res. 35 (11) (2020 Nov) 2159–2170.
[19] D.E. Whittier, L.A. Burt, D.A. Hanley, S.K. Boyd, Sex- and site-specific reference data for bone microarchitecture in adults measured using second-generation HR-pQCT, J. Bone Miner. Res. 35 (2020) 2151–2158.
[20] M.L. Bouxsein, S.K. Boyd, B.A. Christiansen, R.E. Guldberg, K.J. Jepsen, R. Müller, Guidelines for assessment of bone microstructure in rodents using micro-computed tomography, J. Bone Miner. Res. 25 (2010) 1468–1486.
[21] D.E. Whittier, S.K. Boyd, A.J. Burghardt, J. Paccou, A. Ghasem-Zadeh, R. Chapurlat, et al., Guidelines for the assessment of bone density and

microarchitecture in vivo using high-resolution peripheral quantitative computed tomography, Osteoporos. Int. 31 (2020) 1607–1627.
[22] R.A. Hannon, J.A. Clowes, A.C. Eagleton, A. Al Hadari, R. Eastell, A. Blumsohn, Clinical performance of immunoreactive tartrate-resistant acid phosphatase isoform 5b as a marker of bone resorption, Bone 34 (2004) 187–194.
[23] S. Yamada, M. Inaba, M. Kurajoh, K. Shidara, Y. Imanishi, E. Ishimura, et al., Utility of serum tartrate-resistant acid phosphatase (TRACP5b) as a bone resorption marker in patients with chronic kidney disease: independence from renal dysfunction, Clin. Endocrinol. 69 (2008) 189–196.
[24] M. Saito, K. Marumo, Collagen cross-links as a determinant of bone quality: a possible explanation for bone fragility in aging, osteoporosis, and diabetes mellitus, Osteoporos. Int. 21 (2010) 195–214.
[25] P. Afzelius, M.-M. Garding, S. Molsted, Dual-energy X-ray absorptiometry of both hips helps appropriate diagnosis of low bone mineral density and osteoporosis, Diagnostics (Basel). 7 (2017).
[26] S. Bonaretti, S. Majumdar, T.F. Lang, S. Khosla, A.J. Burghardt, The comparability of HR-pQCT bone measurements is improved by scanning anatomically standardized regions, Osteoporos. Int. 28 (2017) 2115–2128.
[27] N. Okazaki, K. Chiba, A.J. Burghardt, C. Kondo, M. Doi, K. Yokota, et al., Differences in bone mineral density and morphometry measurements by fixed versus relative offset methods in high-resolution peripheral quantitative computed tomography, Bone 115973 (2021).
[28] M. Sode, A.J. Burghardt, J.-B. Pialat, T.M. Link, S. Majumdar, Quantitative characterization of subject motion in HR-pQCT images of the distal radius and tibia, Bone 48 (2011) 1291–1297.
[29] J.B. Pialat, A.J. Burghardt, M. Sode, T.M. Link, S. Majumdar, Visual grading of motion induced image degradation in high resolution peripheral computed tomography: impact of image quality on measures of bone density and micro-architecture, Bone 50 (2012) 111–118.
[30] K. Chiba, N. Okazaki, Y. Isobe, S. Miyazaki, A. Yonekura, M. Tomita, et al., Precision of 3D registration analysis for longitudinal study of second-generation HR-pQCT, J. Clin. Densitom. 24 (2) (2021 Apr) 319–329.
[31] T. Hildebrand, P. Rüegsegger, A new method for the model-independent assessment of thickness in three-dimensional images, J. Microsc. 185 (1997) 67–75.
[32] T. Hildebrand, P. Rüegsegger, Quantification of bone microarchitecture with the structure model index, Comput. Methods Biomech. Biomed. Engin. 1 (1997) 15–23.
[33] A. Odgaard, H.J. Gundersen, Quantification of connectivity in cancellous bone, with special emphasis on 3-D reconstructions, Bone 14 (1993) 173–182.
[34] W.J. Whitehouse, The quantitative morphology of anisotropic trabecular bone, J. Microsc. 101 (1974) 153–168.
[35] A. Vesterby, H.J. Gundersen, F. Melsen, Star volume of marrow space and trabeculae of the first lumbar vertebra: sampling efficiency and biological variation, Bone 10 (1989) 7–13.
[36] M. Iki, Y. Fujita, J. Tamaki, K. Kouda, A. Yura, E. Kadowaki, et al., Design and baseline characteristics of a prospective cohort study for determinants of osteoporotic fracture in community-dwelling elderly japanese men: the fujiwara-kyo osteoporosis risk in men (FORMEN) study, BMC Musculoskelet. Disord. 10 (2009) 165.
[37] J.A. Kanis, G. Bianchi, J.P. Bilezikian, J.M. Kaufman, S. Khosla, E. Orwoll, et al., Towards a diagnostic and therapeutic consensus in male osteoporosis, in: Osteoporos Int, Springer-Verlag, 2011, pp. 2789–2798.
[38] P. Szulc, P. Garnero, F. Munoz, F. Marchand, P.D. Delmas, Cross-sectional evaluation of bone metabolism in men, J. Bone Miner. Res. 16 (2001) 1642–1650.
[39] N. Yoshimura, S. Muraki, H. Oka, M. Morita, H. Yamada, S. Tanaka, et al., Profiles of vitamin D insufficiency and deficiency in Japanese men and women: association with biological, environmental, and nutritional factors and coexisting disorders: the ROAD study, Osteoporos. Int. 24 (2013) 2775–2787.
[40] K. Nakamura, K. Kitamura, R. Takachi, T. Saito, R. Kobayashi, R. Oshiki, et al., Impact of demographic, environmental, and lifestyle factors on vitamin D sufficiency in 9084 Japanese adults, Bone 74 (2015) 10–17.
[41] J. Tamaki, M. Iki, Y. Sato, E. Kajita, H. Nishino, T. Akiba, et al., Total 25-hydroxyvitamin D levels predict fracture risk: results from the 15-year follow-up of the japanese population-based osteoporosis (JPOS) cohort study, Osteoporos. Int. 28 (2017) 1903–1913.
[42] A. Kuwabara, N. Tsugawa, K. Mizuno, H. Ogasawara, Y. Watanabe, K. Tanaka, A simple questionnaire for the prediction of vitamin D deficiency in Japanese adults (Vitaimn D Deficiency questionnaire for Japanese: VDDQ-J), Journal of Bone and Mineral Metabolism. 37 (2019) 854–863.
[43] J.S. Thomsen, M.V. Jensen, A.S. Niklassen, E.N. Ebbesen, A. Brüel, Age-related changes in vertebral and iliac crest 3D bone microstructure–differences and similarities, Osteoporos. Int. 26 (2015) 219–228.
[44] H. Chen, X. Zhou, S. Shoumura, S. Emura, Y. Bunai, Age- and gender-dependent changes in three-dimensional microstructure of cortical and trabecular bone at the human femoral neck, Osteoporos. Int. 21 (2010) 627–636.
[45] A.K. Amstrup, N.F.B. Jakobsen, E. Moser, T. Sikjaer, L. Mosekilde, L. Rejnmark, Association between bone indices assessed by DXA, HR-pQCT and QCT scans in post-menopausal women, J. Bone Miner. Metab. 34 (6) (2016 Nov) 638–645.
[46] S.K. Boyd, L.A. Burt, L.K. Sevick, D.A. Hanley, The relationship between serum 25 (OH)D and bone density and microarchitecture as measured by HR-pQCT, Osteoporos. Int. 26 (2015) 2375–2380.